Available online at www.sciencedirect.com
ScienceDirect
Biomaterials 28 (2007) 1998–2009
Biomaterials
www.elsevier.com/locate/biomaterials

One-step fabrication of porous micropatterned scaffolds to control cell behavior

Bernke J. Papenburg, Laura Vogelaar, Lydia A.M. Bolhuis-Versteeg, Rob G.H. Lammertink, Dimitrios Stamatialis*, Matthias Wessling

Department of Science and Technology, Institute for BioMedical Technology (BMTi), Membrane Technology Group, University of Twente, P.O. Box 217, 7500 AE Enschede, The Netherlands

Received 14 September 2006; accepted 31 December 2006
Available online 18 January 2007

Abstract

This paper reports a one-step method to fabricate highly porous micropatterned 2-D scaffold sheets. The scaffold sheets have high glucose diffusion, indicating that the porosity and pore morphology of the scaffolds are viable with respect to nutrient transport, and a micropattern for cell alignment. HUVEC culturing proved that the scaffold sheets are suitable for cell culturing. More extensive culturing experiments with mouse myoblasts, C2C12, and mouse osteoblasts, MC3T3, showed that tissue organization can be controlled; the micropattern design affects the extent of cell alignment and tissue formation. Cells are favorably settled in the micropattern and even at higher confluence levels, when the cells start to overgrow the ridges of the micropattern, these cells align themselves in the direction of the micropattern. Preliminary multi-layer stacking experiments indicate that the 2-D scaffold sheets are very promising as basis for building 3-D scaffolds.

Keywords: Scaffold; Tissue engineering; Phase separation; Micropatterning; Porosity; Cell alignment

1. Introduction

Tissue engineering originates from reconstructive surgery using donor tissue to repair damaged tissue. Direct transplantation of tissue is still the most common method to restore tissue functions. However, direct transplantation of a whole organ or large areas such as skin is often not feasible. Frequently, autogenic transplants are not available and problems of rejection, pathogen transmission and lack of sufficient donor organs are inevitable for allogenic transplants. Therefore, the possibility to provide an autogenic transplant by constructing a tissue-engineered replacement in vitro can be an excellent alternative. Consequently, the last years great efforts have been focused on tissue engineering [1–4].

One of the major themes in tissue engineering is scaffold fabrication. A scaffold is an artificial extra cellular matrix (ECM), which serves as temporary support where isolated cells are introduced to form tissue. The scaffold should be biocompatible, biodegradable, promote cell attachment and should be mechanical stable [5–8]. High porosity and pore connectivity is essential to ensure sufficient nutrient diffusion through the scaffold, i.e., transport of oxygen and nutrients towards the cells and allow metabolic products to be removed [9]. Furthermore, porosity appears to have a positive effect on cell attachment as well [10]. Moreover, early studies suggest micropatterned scaffolds improve tissue formation. Cell attachment and cell orientation are promoted due to guidance of the cells by a patterned microarchitecture, leading to better implants since in vitro tissue which closely mimics in vivo tissue organization will maintain its functionality better. An optimum design of the micropatterned scaffold appears to be crucial for tissue engineering [11–14].

Current fabrication methods do not combine the production of porous scaffolds with pore-sizes in the micrometer-scale and the enclosure of micropatterning.

*Corresponding author. Tel.: +31 534894675; fax: +31 53 4894611.
E-mail address: d.stamatialis@utwente.nl (D. Stamatialis).

0142-9612/$ - see front matter © 2007 Elsevier Ltd. All rights reserved.
doi:10.1016/j.biomaterials.2006.12.023

Several researchers design scaffolds which are only porous using various methods e.g., foaming [15,16], particulate-leaching [17,18], immersion precipitation [19,20] and freeze drying [21,22]. These methods prepare porous scaffolds in geometries like sheets and cubes. Others design only micropatterned scaffolds using various techniques [14,23–25], such as soft lithography. In soft lithography, microcontact printing is commonly used. In this case, an elastomeric 'stamp' (e.g. Poly(dimethyl)-siloxane (PDMS)) is produced to stamp an ink micropattern on the scaffold surface. Subsequently, a coating is often applied on the parts of the surface without ink. Soft lithography requires rigid surfaces for precise patterning which limits the materials that can be used for patterning. Furthermore, all these additional post-processing steps result in a chemically coated surface, which might be unstable on the long-term since serum in the cell culture medium can affect the coating [23,26].

Only recently research has been performed to create porosity into an already prepared dense micropatterned scaffold. This method involved the combination of soft-lithography and melt molding to fabricate the dense micropatterned sheets and post-processing particulate leaching of micro/nanospheres to create pores [27]. Although the diffusion of nutrients through these scaffolds was increased compared to dense scaffolds, the pores appeared to be isolated voids without good interconnectivity.

It is evident that there is need for an easy fabrication method which combines micropattering directly with the fabrication of highly porous scaffolds, resulting in highly improved scaffolds [27]. Additionally, the exact regulation of the pore size of the micropatterned scaffolds is highly significant, too. If the pores have an average size of tens of micrometers or more, the cells will conform to this pore morphology instead of the applied micropattern, leading to decreased cell organization [27]. However, if the pores are too small, nutrient diffusion will be limited. Therefore, an optimal pore-size should be addressed, which depends on various parameters, e.g. the type of cell, and has to be determined experimentally.

In this work, we fabricate scaffolds having both high porosity with controllable micrometer-scale pores and incorporated micropatterns of excellent quality. Our method is called Phase Separation Micromolding (PSμM). In one step, highly porous micropatterned sheets can be obtained due to immersion precipitation of a polymer on a micropatterned mold [28,29]. A great advantage of PSμM is the broad range of pore size, porosity and interconnectivity that can be obtained by fine-tuning the phase separation process parameters. The pore morphology can be tuned such that adequate nutrient diffusion to the cells can be achieved without disturbing the tissue organization induced by the micropattern. Additionally, PSμM enables processing of a large range of materials. The only requirement for a material to be suitable for PSμM is the existence of a solvent and a non-solvent, which is miscible with the solvent [28,29]. Therefore, directly implantable materials can be used as well.

In this study, we use PSμM to prepare in one step micropatterned porous 2-D scaffold sheets using various polymers. The porosity and pore size is tuned for adequate nutrient diffusion and the scaffold sheets control cell organization through micropatterning. A proof-of-principle is presented of multi-layer stacking 2-D scaffold sheets into a 3-D scaffold for tissue engineering.

1.1. Background PSμM

PSμM is a microfabrication method based on immersion precipitation on a micropatterned mold (see Fig. 1) [28,29]. Prior to preparation of the micropatterned polymer sheets, a master mold with a microarchitecture has to be fabricated from a silicon wafer using technologies derived from microelectronics and photolithography [28,29]. PSμM comprises of three parts: (I) Casting a polymer solution onto the mold. (II) Immersing the mold with the polymer solution into the non-solvent bath. Phase separation is initiated due to solvent and non-solvent liquid exchange leading to a situation where the polymer solution contains sufficient non-solvent to precipitate. Solidification of the micropatterned polymer sheet takes place on the mold, where the inverse replication of the micropattern is imprinted in the polymer sheet. (III) The solidified micropatterned polymer sheet is released from the mold.

Many parameters influence the porosity and pore morphology of polymer sheets obtained by immersion precipitation [30,31], e.g. the choice of polymer, solvent and non-solvent, polymer solution concentration, the temperature of the polymer solution and/or the coagulation bath. Concerning tissue engineering, often the average scaffold porosity is evaluated. This can be misleading; some sheets might have relatively high porosity yet might not be suitable for nutrient diffusion mainly due to two key

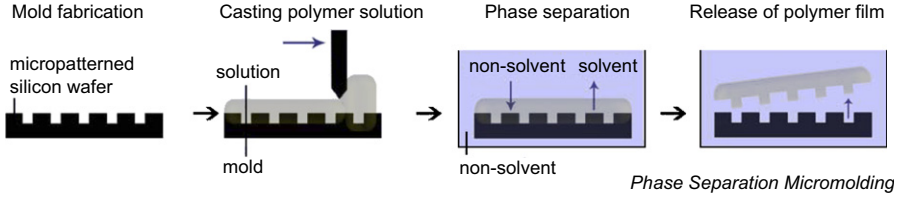

Fig. 1. Schematic illustration of the phase separation micromolding process.

features: non-percolating cellular structure and skin formation. Sheets with a cellular structure contain isolated closed pores, implying low interconnectivity, and sheets containing a skin show a thin dense outer layer limiting the diffusion.

2. Materials and methods

2.1. Micropatterned porous scaffold preparation

Micropatterned sheets were fabricated using various recipes of PSμM. The molecular weight (M_w) of the polymer can have a significant effect on the mechanical properties of the prepared sheets. Sheets prepared by polymers of high M_w usually have better mechanical stability. Therefore, in this study we selected known biocompatible and biodegradable polymers of relatively high M_w. The polymers used were: poly(L-lactic acid) (PLLA, $M_w = 160\,000$ g/mol) kindly provided by Dr. D. Grijpma (University of Twente), poly(D,L-lactic acid) (PDLLA, Polysciences, $M_w = 330\,000$–$600\,000$ g/mol) and poly(ε-caprolactone) (PCL, Solvay (CAPA 680), $M_w = \sim 80\,000$ g/mol). Dioxane and chloroform (both Merck, analytical quality) were used as solvent whereas several alcohols with increasing number of carbon atoms: methanol, ethanol, isopropanol, isobutanol (Merck, analytical quality) and isopentanol (Acros, extra pure) were used as non-solvents. The polymer concentrations of the PLLA and PDLLA polymer solutions were 5, 7.5, and 10 wt%, whereas the PCL polymer solutions were 12.5 and 15 wt%. Generally, the micropatterned sheets were prepared at room temperature ($T = 23 \pm 2$ °C); however, in some cases the temperature of the non-solvent bath was decreased to 4 °C (see details later). The polymer solutions were first casted on the mold and directly placed in the non-solvent bath. After releasing from the mold, the resulting sheets were left in the non-solvent for 1 day to ensure complete removal of the solvent. Subsequently, the sheets were washed thoroughly with Milli-Q water and dried in a controlled atmosphere ($T = 20$–23 °C).

The micropatterned molds were fabricated by silicon micromachining. First, a microarchitecture was designed and a mask was prepared of this design. Then, the mask was used for specific application of photo-resist on a flat silicon wafer, which was subsequently etched to create the micropatterned mold. More detail on fabrication of the molds can be found in [29].

Various micropatterned molds were designed to determine the effect of the patterning on cell growth and alignment. Fig. 2 illustrates the mold whereas Table 1 presents their specifications (c: channel width, h: channel height, r: ridge width). Mold I has no channels/pattern, molds II and III have channels of various dimensions and for mold IV, the ridges are periodically broken up to enable cells in adjacent channels to be in contact.

2.2. Porosity and pore morphology determination

The inner- and surface porosity and pore morphology of the sheets was determined via image analysis using scanning electron microscopy (SEM, JEOL T220 and JEOL 5600LV). Besides image analysis, the porosity of the micropatterned sheets was estimated using the equations:

$$\text{porosity}\ (\%) = \frac{\text{bulk volume}(\text{m}^3) - \text{skeletal volume}(\text{m}^3)}{\text{bulk volume}(m^3)} \times 100, \quad (1)$$

where

$$\text{bulk volume}(\text{m}^3) = \text{width}(m) \times \text{length}(m) \times \text{thickness}(m), \quad (2)$$

$$\text{skeletal volume}(\text{m}^3) = \frac{\text{weight}(\text{g})}{\text{density}(\text{g}/\text{m}^3)}. \quad (3)$$

The density of the polymers was determined by a pycnometer (Micromeritics Accupyc 1330).

2.3. Nutrient transport

Evaluation of the micropatterned sheets as scaffold for tissue engineering was also performed via glucose diffusion experiments. Glucose is one of the nutrients for cells and is, therefore, a representative indicator for nutrient transport through the sheets. Fig. 3 shows a schematic representation of the glucose diffusion device. A 10-fold of the glucose concentration in blood was used in all experiments; 10 g/L (57 mmol/l, SigmaUltra, D-(+)-glucose, 99.5% GC).

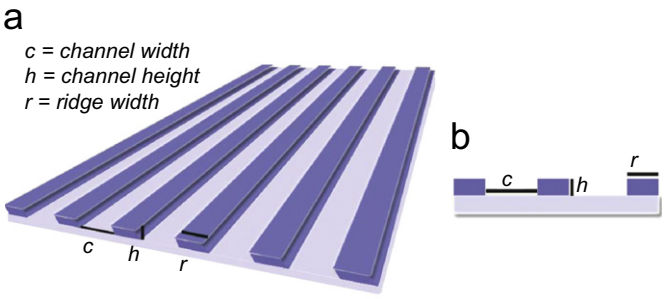

Fig. 2. Schematic illustration of the mold design, (a) top view, (b) side view.

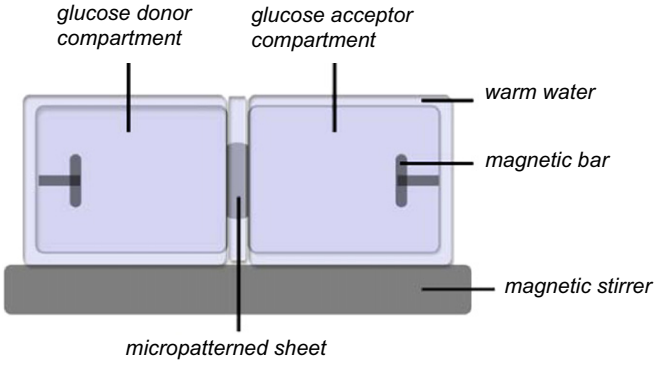

Fig. 3. Schematic representation of the glucose diffusion device.

Table 1
Specifications of the micropatterned molds and the polymer sheet replicas

Mold type	Mold design (μm)			Polymer sheet replication (μm)			Remarks
	c	*h*	*r*	*c*	*h*	*r*	
I	—	—	—	—	—	—	Non-patterned, as reference
II	25	30	25	20	15	25	
III	300	70	50	250	45	40	
IV	20	15	10	16	7	9	Ridges are broken up periodical every 95 μm for 10 μm

One compartment (donor) contained the glucose solution, whereas the other compartment (acceptor) contained pure water. The sheet was placed in the middle of the two compartments. Before starting the experiment, the sheet was pre-wetted for several hours with an ethanol to water gradient to ensure full wetting. Both compartments were double walled and kept at 37 °C with circulating water. At various time intervals, samples of 0.5 ml were taken from both compartments. The glucose concentration was determined using an enzymatic assay (PGO Enzymes, Sigma) [32]. The glucose in the sample reacted with the enzyme, resulting in an orange colored solution. The sample was subsequently analyzed by a UV spectrophotometer (Varian Cary 300 scan) at $\lambda = 450$ nm.

Due to the concentration difference, glucose passes through the sheet from the donor to the acceptor compartment. The amount of glucose that passes through the sheet vs. time is an indication for the porosity and interconnectivity of the sheet. The permeability is a measure for the diffusion in time and can be calculated through the flux using the equation:

$$\text{flux}(\text{g m}^{-2}\,\text{s}^{-1}) = \frac{[(C\text{acceptor}(\text{g m}^{-3}) \times V\text{acceptor}(\text{m}^3))/\text{S}(\text{m}^2)]}{\text{time}(s)}, \quad (4)$$

where C_{acceptor}, the glucose concentration in the acceptor, V_{acceptor}, the volume of the acceptor compartment and S, the surface area of the micropatterned sheet is. The glucose permeability can be calculated:

$$\text{permeability}(\text{m}^2\,\text{s}^{-1}) = \frac{\text{flux}(\text{g m}^{-2}\,\text{s}^{-1})}{\Delta C(\text{g m}^{-3})} \times l(\text{m}), \quad (5)$$

where ΔC is the concentration difference between the donor and the acceptor and l is the average thickness of the micropatterned sheet. From the permeability, the diffusion coefficient can be determined:

$$\text{diffusion coefficient}(\text{m}^2\,\text{s}^{-1}) = \text{permeability}(\text{m}^2\,\text{s}^{-1}) \times K, \quad (6)$$

with K being the partitioning coefficient. Because the glucose molecule is small in comparison to the pore size, K can be assumed to be equal to one.

2.4. Cell culturing

Cell culturing experiments were performed using various cell types. Human umbilical vein endothelial cells (HUVEC) and human microvascular endothelial cells (HMEC) were used in preliminary experiments to determine the effectiveness of the sheets as scaffold material. C2C12 (mouse myoblasts) and MC3T3 (mouse osteoblasts) cells were used to study the influence of the micropattern on cell alignment and tissue formation.

Culturing: The micropatterned scaffold sheets were placed in 24-well-plates (Corning Inc., Costar 3526), an o-ring (Viton, type 51414, 14 × 1) of exactly the inner diameter of the well was placed on top of each sheet to keep the scaffolds down to the bottom of the well. Then, the scaffold sheets were sterilized with ethanol and isopropanol and subsequently washed and pre-wetted with phosphate buffer saline (PBS) solution. Cells were trypsinized from a culture flask and diluted with medium to the desired concentration. The cells were added on top of the micropatterned sheets at a cell density of 40.000 (HUVEC and HMEC) or 25 000 cells/cm^2 (C2C12 and MC3T3). The medium used for HUVEC/HMEC was 1:1 RPMI 1640/M 199 supplemented with 1% Pen/Strep, 1% glutamax and 20% human serum. For C2C12, the medium was DMEM supplemented with 1% Pen/Strep and 10% FBS. Medium used for MC3T3 was α-MEM supplemented with 1% Pen/Strep, 1% L-glutamine, 1% Sodium Pyruvate and 10% FBS. Every 2–3 days, the medium was renewed. The cell-cultured sheets were kept in an incubator at 37 °C and 5% CO_2 for several days (varied between 2 and 10 days).

Fixation and staining: The cells were fixated for at least 30 min using a 4%-formaldehyde solution. After fixation, the C2C12/MC3T3 cultured scaffold sheets were stained by methylene blue for light-microscopy. After adding methylene blue for approx. 5 min, the sheets were washed 3 times with PBS before analysis. For confocal fluorescence microscopy, the scaffold sheets were washed with PBS directly after fixation. Subsequently, the cells were permeabilized by a 0.1% triton-X100 solution for 1 min, washed with PBS and incubated with a 0.05% Bodipy-phallacidine solution (Molecular probes) for 10 min to label the cell cytoskeleton. After washing with PBS, the scaffold sheets were ready for analysis.

Analysis: The HUVEC/HMEC cultured scaffold sheets were analyzed by light microscopy (Zeiss Axiovert 40 mat and Axiocam MRc 5 camera) during the cell culture without harming the cells.

The C2C12/MC3T3 cell-cultured sheets were analyzed by light microscopy and complementary with confocal fluorescence microscopy (Zeiss LSM 510). To determine the extent of alignment, a grid was projected on the confocal fluorescence microscopy images [33,34]. One axis (Y) of the grid ran parallel to the channels, where the other axis (X) ran perpendicular to the channels. The extent of alignment was calculated determining the amount of cells crossing the grid lines:

$$\text{alignment}(\%) = \frac{X - Y}{X + Y} \times 100. \quad (7)$$

For a 3-D scaffold, nutrient transport through the scaffold should be enabled by the inner-porosity. In addition to the glucose diffusion experiments, a culturing experiment was performed to simulate nutrient diffusion through the scaffold sheet. Scaffold sheets of exactly the size of the inner diameter of a well (24-well plate) were prepared. Subsequently, C2C12 cells were seeded on the micropattern (see method described previously). After approximately 3 h attaching of the cells, half of the cell-cultured sheets were turned up side down in the wells. The o-ring was placed tightly on top of each sheet to ensure that no leakage of nutrients via the sides would take place. In this case, nutrient supply to the cells can only be achieved by nutrient transport through the inner-porosity of the sheets. After 2 and 4 days, the turned sheets were compared to the reference sheets where the cells were in direct contact to the medium and oxygen (fixation, staining and analysis described previously).

2.5. 3-D scaffolds proof-of-principle

The 2-D micropatterned sheets can be built into a 3-D scaffold by multi-layer stacking immediately after casting. Then, residues of the solvent are still present in the sheets enabling the layers to bond. Stacking was achieved through two different methods: by either clamping several films between glass-plates or rolling up one or more sheets around a tube. Through the combination of pressure applied and softened material, the layers bond. After clamping or rolling up, the sheets were left in the non-solvent bath for one day. Subsequently, the sheets were washed thoroughly with water (milli-Q) and dried in a controlled atmosphere after which, in case of clamping, the glass-plates were removed. Both methods achieve firm contact of the sheets.

3. Results and discussion

3.1. Micropatterned sheet preparation

In order to determine the effect of the microarchitecture on cell behavior, various molds were fabricated from silicon wafers. Table 1 presents the dimensions (length, width, dept) of the designed microarchitectures of the master molds. The molds featuring the different micropattern designs are indicated in the rest of the text as type I–IV (see details Table 1). Using PSμM, polymer replicas were prepared. Table 1 presents the dimensions of these replicas as well. Since low polymer concentrations were used, the shrinkage during the phase separation process was significant. In fact, the micropattern dimensions of the polymer sheet surface were up to 20% smaller compared to the master mold design where the channel dept shrunk up

to 50%. The shrinkage was taken into account when designing the master mold, therefore, it was well controlled and the replicated features were of very good quality. Besides, the shrinkage helps easy release of the sheet from the mold.

3.2. Porosity and pore morphology determination

Fig. 4 shows typical SEM pictures of the wide variety of prepared morphologies, varying from very dense to very porous depending on the recipe. For three different polymers the effect of various parameters, i.e. solvent, polymer concentration and non-solvent, was determined. Table 2 represents the results of the porosity of the various structures determined by Eqs. (1)–(3). As mentioned in the remarks of Table 2, in some cases cellular structure and/or skin formation was observed. Both characteristics are disadvantageous since they will lead to decreased nutrient transport through the sheet.

PLLA: In the case of PLLA, the solvent has a significant effect on the porous structure. Dioxane appears most suitable as solvent since higher porosities and generally higher pore size is obtained in comparison to chloroform (Table 2). Since dioxane is less volatile compared to chloroform, the evaporation rates are decreased. Therefore, the solidification is delayed and the film has less skin formation and higher overall porosity. When increasing the PLLA concentration from 5 to 7.5 and 10 wt% in dioxane, the sheet becomes less porous (Table 2). Finally, the effect of the different alcohols as non-solvents seems to be marginal in terms of porosity. However, the quality of the structure was better for ethanol and isopropanol.

More experiments were performed to optimize the structure of these sheets. In these experiments, the temperature of the non-solvent bath was decreased to 4 °C. This had an extensive impact on the skin formation of the sheets leading to significantly higher surface porosity and probably pore-interconnectivity. Fig. 4a–c presents very porous structures obtained for PLLA-dioxane sheets using these two non-solvents at 4 °C.

PDLLA: In the case of PDLLA, the solvent and non-solvent have a significant effect on the sheet structure. With either chloroform or dioxane as solvent and methanol as non-solvent, the structure is non-porous (Table 2 and Fig. 4d–f). For dioxane, porosity of only 28% can be achieved when ethanol and isopropanol are used as non-solvents, which is probably due to pore collapse during solidification (Table 2). For chloroform, however, a porosity of ~64% can be achieved using these alcohols as non-solvent, although a dense skin was formed.

PCL: PCL sheets could not be prepared at polymer concentrations lower than 10 wt%. Due to the high polymer content, less polymer lean phase is formed resulting in rather moderate porosity of 51.7% (Table 2).

Considering the purpose of the sheets as scaffolds, and the accompanying requirements, sheets prepared from 5 wt% PLLA in dioxane solutions with the non-solvent bath at 4 °C show the most promising features, i.e., high porosity and probably pore-interconnectivity. Estimation of the porosity by calculation does not always give the best insight into the real porosity and most importantly pore-interconnectivity, which are highly important with respect to nutrient diffusion limitations. Therefore, these 5 wt% PLLA-dioxane scaffolds were examined in more detail with regard to nutrient transport.

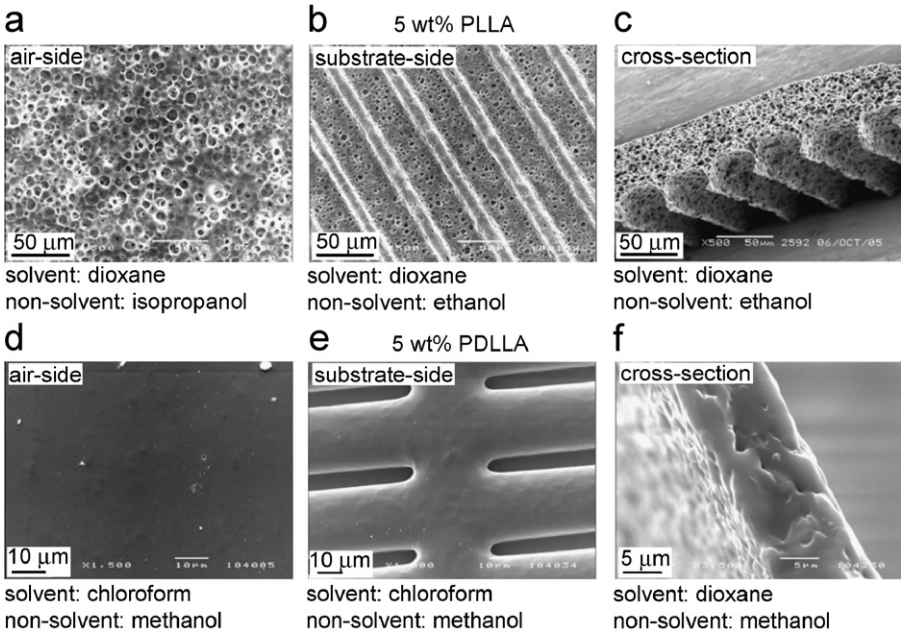

Fig. 4. Typical SEM pictures of films obtained by PSμM indicating broad porosity that can be obtained (a–c) non-solvent at 4 °C, (d–f) non-solvent at 23 °C.

Table 2
Porosity determination various films prepared by PSμM

Polymer	Solvent	wt%	Non-solvent	Porosity (%)	Average porosity (%)	Pore size range (μm)	Remarks
PLLA	Chloroform	5	Ethanol	55.2	61.6	2–4	Cellular and skin
			Isopropanol	67.9		2–4	
PLLA	Dioxane	5	Methanol	82.1	81.3	5–6	Good quality structures
			Ethanol	78.9		5–8	
			Isopropanol	83.9		5–9	
			Isobutanol	79.9		5–9	
			Isopentanol	81.7		2–10	
PLLA	Dioxane	7.5	Ethanol	75.9	75.7	1–3	Good quality structures
			Isopropanol	75.5		2–5	
PLLA	Dioxane	10	Ethanol	61.9	70.3	3–4	Good quality structures
			Isopropanol	78.6		2–4	
PDLLA	Chloroform	5	Methanol	no	no	—	Dense
			Ethanol	63.7	64.0	0.2–1.5	Cellular and skin
			Isopropanol	64.2		0.5–1.5	
PDLLA	Dioxane	5	Methanol	no	no	—	Dense
			Ethanol	28.3	28.2	0.2–2	Collapsed pores
			Isopropanol	28.0		0.2–1	
PCL	Chloroform	12.5	Ethanol	47.1	51.7	3–13	Cellular and skin
			Isopropanol	56.3		5–13	

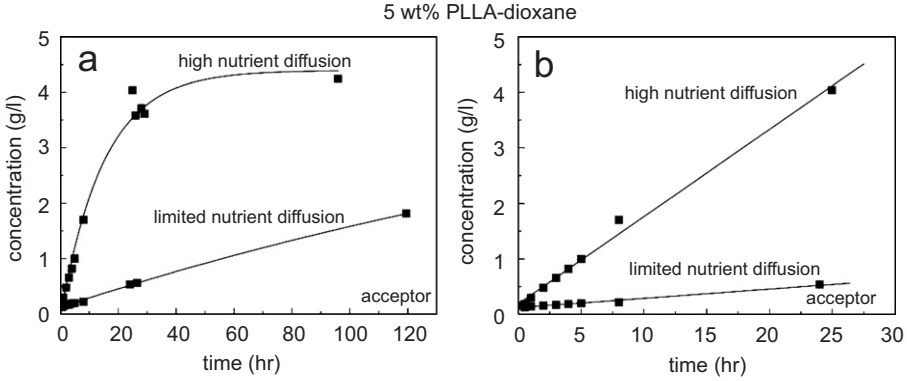

Fig. 5. Typical graphs of glucose diffusion towards the acceptor as function of time; high nutrient diffusion: 29 μm thick sheet prepared with isopropanol as the non-solvent at 4 °C, limited nutrient diffusion: 52 μm thick sheet prepared with ethanol as the non-solvent at 23 °C. (a) 96 h, (b) zoom at the first 24 h.

3.3. Nutrient transport

Fig. 5 shows typical results of glucose diffusion in time through a 5 wt% PLLA-dioxane sheet. Fig. 5a shows the transport over a period of 96 h, whereas Fig. 5b focuses on the first 24 h. In both graphs, the results of two different sheets are displayed. One is porous and interconnected, where high diffusion is reached (sheet prepared by isopropanol as the non-solvent at 4 °C). The second is denser or has lower pore-interconnectivity limiting the nutrient transport (sheet prepared by ethanol as the non-solvent at 23 °C). The glucose transport was rather linear at low time period (up to 24 h). Subsequently, the glucose concentration difference between donor and acceptor decreases and the concentration reaches a plateau. Table 3 presents the glucose diffusion coefficients for various sheets prepared using a 5 wt% PLLA-dioxane solution, determined by Eqs. (4)–(6). Parameters that were altered are the non-solvent (ethanol or isopropanol), initial casting thickness (100 and 200 μm) and the temperature of the non-solvent bath (room temperature, i.e. ~23 or ~4 °C). Due to the low polymer concentration in the

Table 3
Glucose diffusion through sheets prepared by a 5 wt% PLLA in dioxane solution (using a glucose solution of 10 g/l)

Non-solvent	$d_{inintial}/d_{real}$ (μm)	$T_{non\text{-}solvent}$ (°C)	Porosity (%)	Diffusion coefficient (10^{-11} m^2/s)[a]
Ethanol	200/52	23	84.3±2.1	1.5±0.5
	100/27	23	82.6±0.7	3.3±0.1
	100/21	4	75.2±1.6	10.4±4.5
Isopropanol	200/57	23	86.0±0.8	2.6±0.2
	100/36	23	86.0±1.2	6.4±1.7
	100/29	4	83.0±2.6	8.6±1.5

[a]Free diffusion of glucose in water (or saline) at 37 °C is 90×10^{-11} m^2/s [35].

polymer solution, the sheets shrink extensively during solidification. Therefore, the final (real) sheet thickness is mentioned as well (Table 3). Although porosity is a good estimation of nutrient diffusion through a sheet, it does not comprehend the existence of a dense skin layer and/or pore-interconnectivity. These phenomena have a major impact on the diffusion of glucose through the sheet.

For both ethanol and isopropanol as non-solvents, it seems that the initial casting thickness has an effect on the sheet structure. When the initial casting thickness becomes half (200–100 μm), the glucose diffusion coefficient is doubled (in the calculations, the real thickness of the sheet is used and the diffusion coefficient should generally not change with thickness). Therefore, this increase in the diffusion coefficient indicates that the structure and/or interconnectivity of the sheet are influenced by the initial casting thickness. For the thicker films (casting thickness 200 μm), even though the calculated porosity does not differ from the thinner ones (casting thickness 100 μm), the pore-interconnectivity is probably lower resulting into lower glucose diffusion.

When subsequently the temperature of the non-solvent bath is decreased from room temperature (~23 °C) to ~4 °C, the final thickness is decreased more probably due to decreasing pore size. However, decreasing the non-solvent bath temperature also causes a significant increase of surface porosity (removal of skin). This effect might counterbalance the overall porosity change. Therefore, with a decrease of the non-solvent bath temperature from room temperature to ~4 °C, the diffusion of glucose increases significantly (for ethanol more severely compared to isopropanol). For the non-solvent bath at room temperature, isopropanol results in higher diffusion compared to ethanol. For the non-solvent bath at ~4 °C, ethanol leads to higher diffusion coefficients compared to isopropanol.

For the most optimal sheets, i.e., prepared from 5 wt% PLLA-dioxane solution and the non-solvent at 4 °C, the glucose diffusion coefficient is $8\text{–}10 \times 10^{-11}$ m^2/s and rather close to the self diffusion of glucose in water or saline solution which is 90×10^{-11} m^2/s [35]. This result is very promising, since the high glucose diffusion through the scaffold sheets implies that the porosity and pore-interconnectivity are most likely adequate for sufficient nutrient supply to the cells.

3.4. Cell culturing

Sheets prepared from a 5 wt% PLLA-dioxane solution using ethanol or isopropanol as the non-solvent, at both room temperature and ~4 °C, showed the most optimal results considering pore-morphology and interconnectivity and were used in cell culturing. It is often argued that the phase separation process can lead to sheet formation where residues of the toxic solvents (as dioxane in our case) and/or non-solvent remain. In order to evaluate the sheets as scaffold material, preliminary culturing experiments were performed using HUVECs and HMECs. These results (not shown here) showed high affinity of the cells to the material (good cell growth was observed) indicating no solvent or non-solvent remained and these sheets are suitable as scaffold material. Moreover, the non-solvents (i.e., ethanol and isopropanol) are sterilizing agents, which is an additional advantage. More extensive experiments on the influence of patterning on cell alignment were performed using C2C12 and MC3T3 cells. The cell-cultured sheets were analyzed by light-microscopy and subsequently with confocal fluorescence microscopy to observe the quality of the tissue formation by cytoskeleton staining (Fig. 6).

Cell culturing on micropatterned scaffold sheets induces alignment of both the C2C12 as well as the MC3T3 cells, and the level of orientation is influenced by the micro-pattern design. Fig. 7 presents the extent of alignment of C2C12 cells for the various micropatterned sheets in comparison to non-patterned sheets, calculated by Eq. (7). As expected, the non-patterned reference samples (type I) showed a random orientation of the cells (Fig. 6a, b). Sheets featuring 20 μm wide channels (type II) showed high orientation of 81±5% (Fig. 6c,d). When the channels are wide (250 μm, Fig. 6e, f) the orientation of the cells was lower (58±6%). The cells aligned in the direction of the channels, although within the wide channels, the individual cells showed a slightly higher variation in orientation compared to the 20 μm wide channels (see confocal fluorescence microscopy, Fig. 6f). Fig. 6g,h show cells

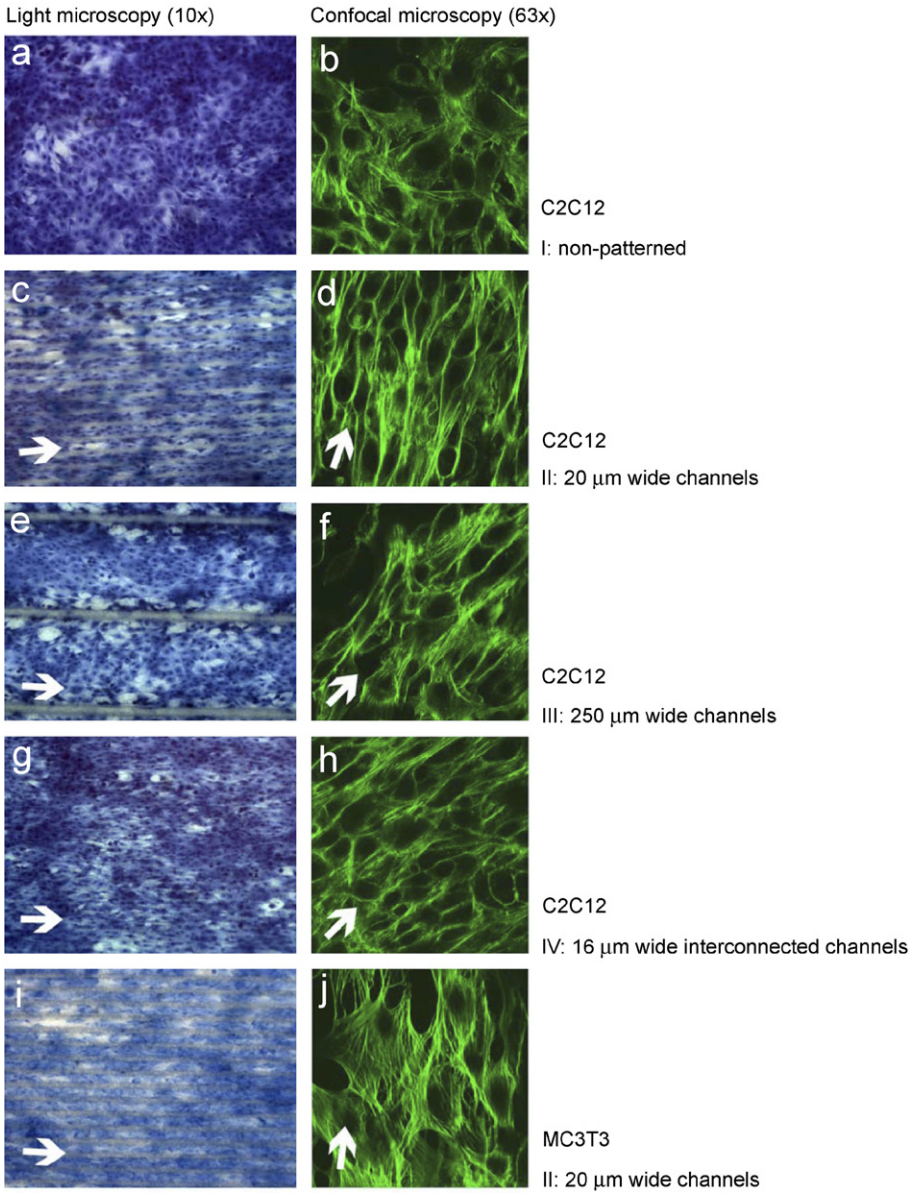

Fig. 6. Typical pictures of culturing cells on PLLA sheets featuring different patterns, after 4 days, seeding density of 25 000 cells/cm^2. The arrows indicate channel direction. (a, c, e, g, i) light microscopy (magnification 10 ×, methylene blue used for staining), (b, d, f, h, j) confocal fluorescence microscopy (magnification 63 ×).

grown on sheets featuring interconnected 16 μm wide channels (type IV) with good cell alignment as well; 64 ± 1%. In this case, due to connections between the channels, the cells in adjacent channels are in contact leading to lower alignment compared to continuous channels of approximately the same width (i.e., 20 μm, type II). Confocal fluorescence microscopy images show that the cells grow through these connections.

It is important to note that for samples containing lower cell numbers, the cells are favorably settled in the channels. Only at higher confluence (i.e., more days of culturing), the cells start to overgrow the ridges of the micropattern. Nevertheless, the overgrowing cells are still well aligned in the direction of the micropattern channels. Fig. 8 shows confocal fluorescence microscopy pictures at various depths of tissue grown in the micropatterns of a scaffold type II (20 μm channels). Fig. 8a shows cells grown on the bottom of the channels, where Fig. 8b shows cells halfway the dept of the channels. Fig. 8c shows cells grown directly on top of the micropattern. Fig. 8d and e show cells in the overgrowing layers. In all cases, the cell alignment is clear. The various micropattern designs induce cell alignment; consequently, the formation of the *in vitro* tissue is stimulated to mimic *in vivo* tissue organization. This alignment is known to be advantageous for the tissue quality [10,11].

To determine directly if the nutrient transport through the inner-porosity of the sheets is sufficient for cells to

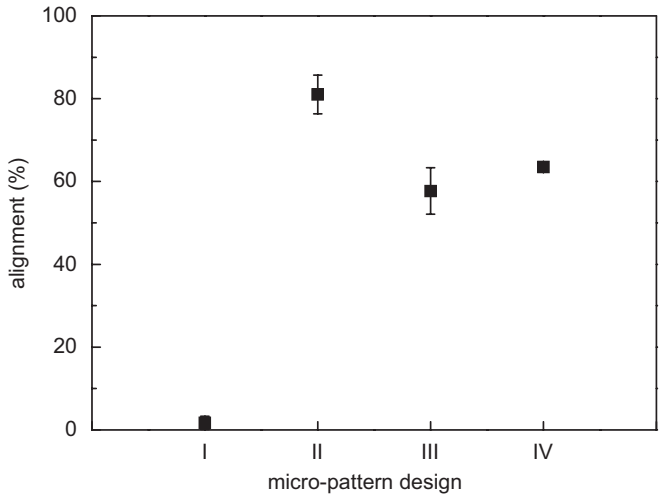

Fig. 7. Extent of cell alignment on sheets featuring various micropattern designs.

proliferate, sheets were turned up side down. In this case, the nutrients have to diffuse through the scaffold sheet to reach the cells. These turned sheets were compared to a reference where the cells were in direct contact to the medium and oxygen. Fig. 9 presents results after 2 and 4 days of culturing for the turned micropatterned sheets (type III), Fig. 9a, c, respectively, and the references, Fig. 9b, d, respectively. These images support the concept that the interconnected porous scaffold sheets enable sufficient nutrient transport through one scaffold sheet for cell proliferation; the number of cells on both the turned and reference scaffold sheets are comparable.

Our results show that PSμM is an excellent method to prepare highly porous micropatterned scaffold sheets with sufficient nutrient diffusivity for cell proliferation, high cell alignment and good tissue formation, even for multiple cell layers.

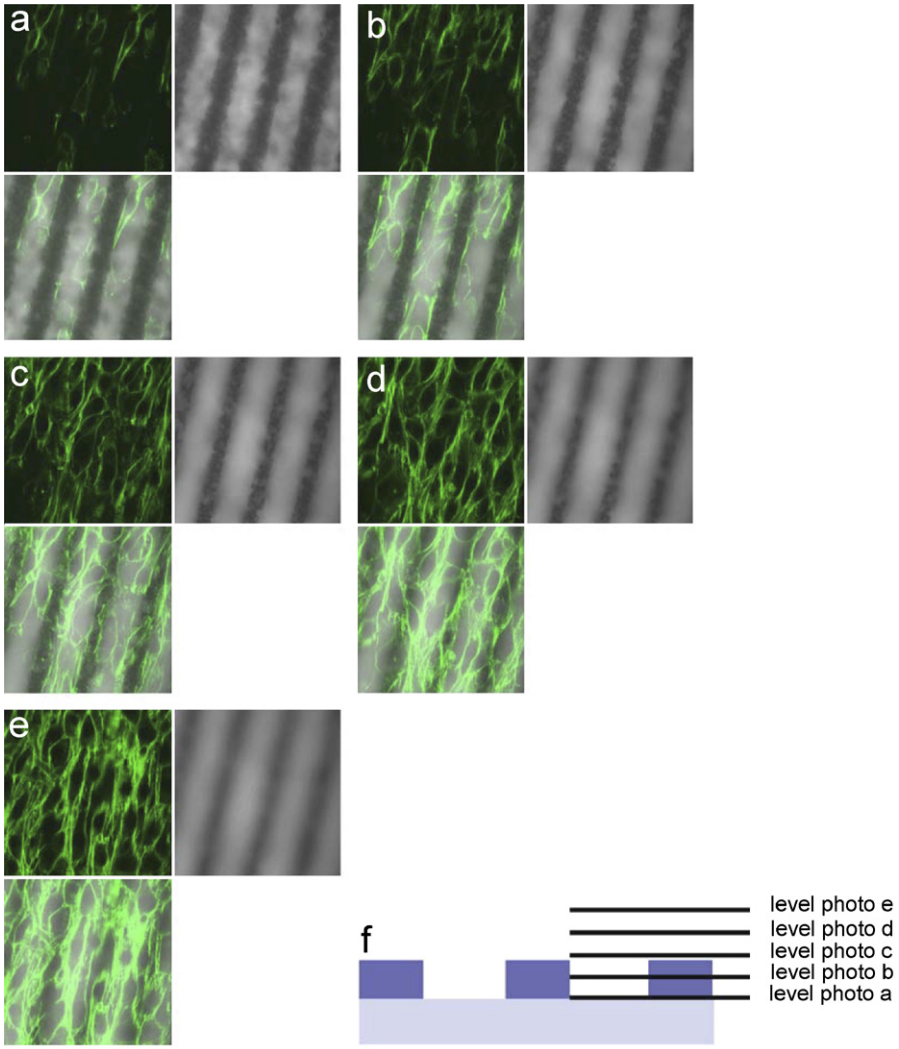

Fig. 8. C2C12 cells overgrowing 20 μm wide micropattern channels (after 4 days of culturing, seeding density of 25 000 cells/cm^2) at various depths of the micropattern; (a–e) upper left picture is taken with confocal fluorescence microscopy, upper right picture is taken with light microscopy on exactly the same place of the sample, lower left is the super-positioned picture of the confocal fluorescence microscopy and light microscopy picture, (f) illustration of the various depth levels of the cells displayed in (a–e) with respect to the micropattern height.

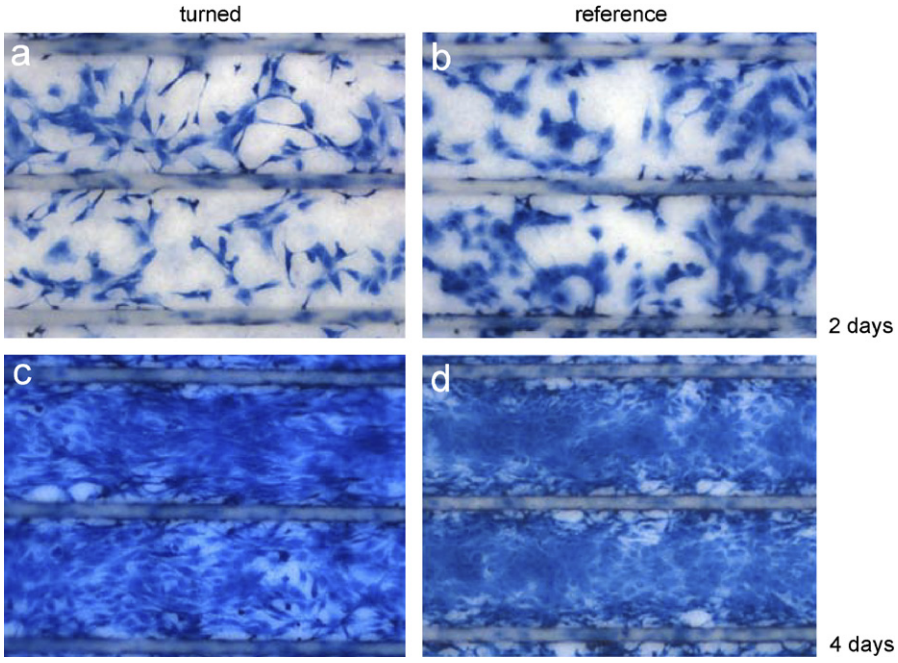

Fig. 9. Light microscopy images of C2C12 cells on micropatterned scaffold sheets containing 250 μm wide channels after 2 (a, b) and 4 (c, d) days of culturing (seeding density 25 000 cells/cm^2); (a, c) scaffold sheets turned around to determine nutrient transport through the sheet towards the cells; (b, d) reference where cells were in direct contact to the nutrients.

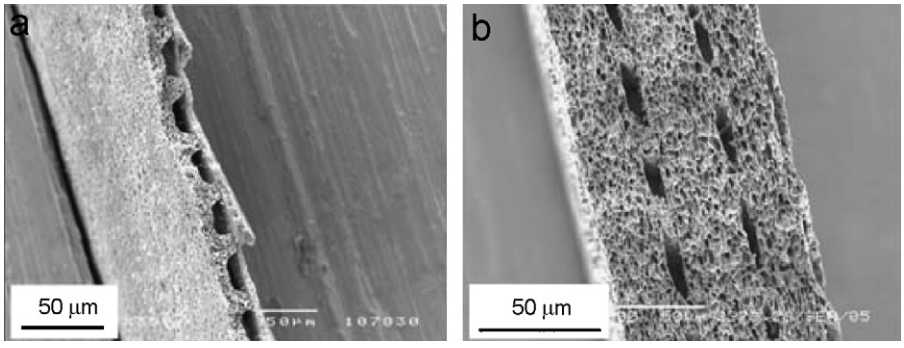

Fig. 10. Stacking scaffold sheets as proof-of-principle of 3-D scaffold design through (a) clamping two films, (b) rolling up one film.

3.5. 3-D scaffolds proof-of-principle

The micropatterned sheets can build 3-D scaffolds by multi-layer stacking of the 2-D sheets. Fig. 10a and b present stacked layers through clamping and rolling up, respectively. In contrast to clamping, in the rolling up process no extensive pressure is applied on the polymer sheets and possible damage to the inner-structure of the sheets can be avoided. By tuning the size of the channels and the sheet thickness, the scaffold architecture can be designed. Although only a few layers have been stacked up till now, the outcome seems promising for stacking more layers into an optimized 3-D scaffold.

In this concept, the channels of the 3-D scaffold can be used for two purposes; either growing cells aligned in the direction of the channels as presented in 2-D and/or for extra nutrient supply to the cells by perfusion. The inner-porosity should ensure nutrient transport of the nutrient supplying layers to the cell-growing layers. Interference of possible nutrient limitations on the quality of cell proliferation has not been studied yet. Therefore, nutrient limitations occurring in 3-D scaffolds containing a higher number of sheets, and how nutrient-supplying layers can assist, will be subject of further research. Then, the maximum nutrient diffusivity path length [36] can be taken into account in the 3-D scaffold design.

4. Conclusion

Phase separation micromolding is an easy method to design micropatterned porous 2-D scaffold sheets in one step. Through fine-tuning of various parameters, highly interconnected porous scaffold sheets can be prepared with

high nutrient diffusivity. Cell culturing of various cell types demonstrates that the micropatterned sheets are suitable as scaffold and good cell attachment and tissue formation can be obtained. Cell alignment is induced by the micropattern, where the level of orientation can be influenced by adjusting micropattern feature and dimensions. Cells are favorably settled in the channels. Even at higher confluence levels where cells start to overgrow the ridges of the micropattern, these cells align themselves in the direction of the channels. The micropatterned sheets are very promising as basis for building a 3-D scaffold with respect to porosity, interconnectivity and control of tissue orientation.

Acknowledgment

The authors would like to thank: D. Grijpma and A. Poot (Polymer Chemistry and Biomaterials Group, University of Twente, The Netherlands) for supplying the polymers and for fruitful discussions; I. van den Brink, J. Boer, and C. van Blitterswijk (Polymer Chemistry and Biomaterials Group, University of Twente, The Netherlands) for technical assistance and guidance concerning the cell culturing experiments; H.-J. Van Manen for technical assistance concerning confocal fluorescence microscopy. This project is supported by the Spearhead program: 'Advanced Polymeric Microstructures for Tissue Engineering' of the University of Twente (BMTi, Institute for Biomedical Technology) and the Dutch Program for Tissue Engineering (DPTE).

References

[1] Levenberg S, Langer R, Gerald PS. Advances in tissue engineering. Curr Topics Dev Biol 2004;61:113–34.
[2] Takezawa T. A strategy for the development of tissue engineering scaffolds that regulate cell behavior. Biomaterials 2003; 24(13):2267–75.
[3] Fuchs JR, Nasseri BA, Vacanti JP. Tissue engineering: a 21st century solution to surgical reconstruction. Ann Thorac Surg 2001;72:577–91.
[4] Langer R, Vacanti JP. Tissue engineering. Science 1993;260:920–6.
[5] Ma PX. Scaffolds for tissue fabrication. Mater Today 2004; 7(5):30–40.
[6] Yeong W-Y, Chua C-K, Leong K-F, Chandrasekaran M. Rapid prototyping in tissue engineering: challenges and potential. Trends Biotechnol 2004;22(12):643–52.
[7] Agrawal CM, Ray RB. Biodegradable polymeric scaffolds for musculoskeletal tissue engineering. J Biomed Mater Res 2001;55(2):141–50.
[8] Hutmacher DW. Scaffolds in tissue engineering bone and cartilage. Biomaterials 2000;21(24):2529–43.
[9] Yang S, Leong K-F, Du Z, Chua C-K. The design of scaffolds for use in tissue engineering. Part I. Traditional factors. Tissue Eng 2001;7(6):679–89.
[10] Hollister SJ. Porous scaffold design for tissue engineering. Nature Mater 2005;4:518–24.
[11] Andersson H, Berg Avd. Microfabrication and microfluidics for tissue engineering: state of the art and future opportunities. Lab on a Chip 2004;4:98–103.
[12] Snyder JD, Desai TA. Fabrication of multiple microscale features on polymer surfaces for applications in tissue engineering. Biomed Microdevices 2001;3(4):293–300.
[13] Desai TA. Micro- and nanoscale structures for tissue engineering constructs. Med Eng Phys 2000;22(9):595–606.
[14] Flemming RG, Murphy CJ, Abrams GA, Goodman SL, Nealey PF. Effects of synthetic micro- and nano-structured surfaces on cell behavior. Biomaterials 1999;20(6):573–88.
[15] Kim TK, Yoon JJ, Lee DS, Park TG. Gas foamed open porous biodegradable polymeric microspheres. Biomaterials 2006; 27(2):152–9.
[16] Wang X, Li W, Kumar V. A method for solvent-free fabrication of porous polymer using solid-state foaming and ultrasound for tissue engineering applications. Biomaterials 2006;27(9):1924–9.
[17] Katoh K, Tanabe T, Yamauchi K. Novel approach to fabricate keratin sponge scaffolds with controlled pore size and porosity. Biomaterials 2004;25(18):4255–62.
[18] Ma PX, Choi J-W. Biodegradable polymer scaffolds with well-defined interconnected spherical pore network. Tissue Eng 2001;7(1):23–33.
[19] Kim SY, Kanamori T, Noumi Y, Wang O-C, Shinbo T. Preparation of porous poly(D,L-lactide) and poly(D,L-lactide-*co*-glycolide) membranes by a phase inversion process and investigation of their morphological changes as cell culture scaffolds. J Appl Polym Sci 2004;92:2082–92.
[20] Zoppi RA, Contant S, Duek EAR, Marques FR, Wada MLF, Nunes SP. Porous poly(L-lactide) films obtained by immersion precipitation process: morphology, phase separation and culture of VERO cells. Polymer 1999;40(12):3275–89.
[21] Ho M-H, Kuo P-Y, Hsieh H-J, Hsien T-Y, Hou L-T, Lai J-Y, et al. Preparation of porous scaffolds by using freeze-extraction and freeze-gelation methods. Biomaterials 2004;25(1):129–38.
[22] O'Brien FJ, Harley BA, Yannas IV, Gibson L. Influence of freezing rate on pore structure in freeze-dried collagen-GAG scaffolds. Biomaterials 2004;25(6):1077–86.
[23] Falconnet D, Csucs G, Michelle Grandin H, Textor M. Surface engineering approaches to micropattern surfaces for cell-based assays. Biomaterials 2006;27(16):3044–63.
[24] Gadegaard N, Martines E, Riehle MO, Seunarine K, Wilkinson CDW. Applications of nano-patterning to tissue engineering. Microelectr Eng 2006;83(4–9):1577–81.
[25] Vozzi G, Flaim C, Ahluwalia A, Bhatia S. Fabrication of PLGA scaffolds using soft lithography and microsyringe deposition. Biomaterials 2003;24:2533–40.
[26] Lussi JW, Falconnet D, Hubbell JA, Textor M, Csucs G. Pattern stability under cell culture conditions—a comparative study of patterning methods based on PLL-*g*-PEG background passivation. Biomaterials 2006;27(12):2534–41.
[27] Sarkar S, Lee GY, Wong JY, Desai TA. Development and characterization of a porous micro-patterned scaffold for vascular tissue engineering applications. Biomaterials 2006;27(27): 4775–82.
[28] Vogelaar L, Lammertink RGH, Barsema JN, Nijdam W, Bolhuis-Versteeg LAM, Rijn CJMv, et al. Phase separation micromolding: a new generic approach for microstructuring various materials. Small 2005;1(6):645–55.
[29] Vogelaar L, Barsema JN, Rijn CJMv, Nijdam W, Wessling M. Phase separation micromolding—PSμM. Adv Mater 2003;15(16):1385–9.
[30] Stropnik C, Musil V, Brumen M. Polymeric membrane formation by wet-phase separation; turbidity and shrinkage phenomena as evidence for the elementary processes. Polymer 2000;41(26): 9227–37.
[31] Witte Pvd, Dijkstra PJ, vandenBerg JWA, Feijen J. Phase separation processes in polymer solutions in relation to membrane formation. J Membr Sci 1996;117(1–2):1–31.
[32] Alexandre E, Schmitt B, Boudjema K, Merrill EW, Lutz PJ. Hydrogel networks of poly(ethylene oxide) star-molecules supported by expanded polytetrafluoroethylene membranes: characterization,

biocompatibility evaluation and glucose diffusion characteristics. Macromol Biosci 2004;4:639–48.
[33] Sarkar S, Dadhania M, Rourke P, Desai TA, Wong JY. Vascular tissue engineering: microtextured scaffold templates to control organization of vascular smooth muscle cells and extracellular matrix. Acta Biomater 2005;1:93–100.
[34] Motlagh D, Hartman TJ, Desai TA, Russell B. Microfabricated grooves recapitulate neonatal myocyte connexin43 and N-cadherin expression and localization. J Biomed Mater Res A 2003;67A(1): 148–57.
[35] Saltzman WM. Tissue engineering: principles for the design of replacement organs and tissues, 1st ed. Oxford: Oxford University Press; 2004.
[36] Dunn JCY, Chan W-Y, Cristini V, Kim JS, Lowengrub J, Singh S, et al. Analysis of cell growth in three-dimensional scaffolds. Tissue Eng 2006;12(4):705–16.